Supporting Information

Flexibility control in alkyl ether-functionalized pillared-layered MOFs by a Cu/Zn mixed metal approach

Andreas Schneemann,[a,b] Robin Rudolf,[c] Samuel J. Baxter,[d] Pia Vervoorts,[a] Inke Hante,[a] Kira Khaletskaya,[a] Sebastian Henke,[c] Gregor Kieslich[b] and Roland A. Fischer[b]

[a]*Lehrstuhl für Anorganische Chemie II, Organometallics and Materials Chemistry, Ruhr-Universität Bochum, Universitätsstr.150, 44780 Bochum, Germany*

[b]*Department of Chemistry, Technische Universität München, Lichtenbergstrasse 4, D-85748 Garching, Germany and Catalysis Research Centre, Technische Universität München, Ernst-Otto-Fischer Strasse 1, 85748 Garching, Germany*

[c]*Anorganische Chemie, Technische Universität Dortmund, Otto-Hahn Straße 6, 44227 Dortmund, Germany*

[d]*School of Chemistrz and Biochemistry, Georgia Institute of Technology, Atlanta, Georgia 30332, United States*

Email: Gregor.Kieslich@tum.de

Roland.Fischer@tum.de

Contents

S1 MOF and Linker Synthesis

The linker was prepared via Williamson ether synthesis of dimethyl-2,5-dihydroxy-1,4-benzenedicarboxylate with 1-bromo-2-methoxyethane. Detailed synthesis procedures have been published elsewhere.[1]

Summary of Synthesis Conditions for the MOF synthesis

Table S1: Summary of synthesis conditions for mixed metal MOFs.

Sample	Sum Formula	m($Zn(NO_3)_2 \cdot 6H_2O$)	m($Cu(NO_3)_2 \cdot 3H_2O$)	m(dabco)
Zn75Cu25	$Zn_{1.5}Cu_{0.5}$(BME-bdc)$_2$(dabco)	187.5 mg	50.5 mg	94 mg
Zn50Cu50	Zn_1Cu_1(BME-bdc)$_2$(dabco)	125 mg	101.5 mg	94 mg
Zn25Cu75	$Zn_{0.5}Cu_{1.5}$(BME-bdc)$_2$(dabco)	62.5 mg	152 mg	94 mg

^{1}H NMR of **Zn75Cu25** (200 MHz, DCl/D_2O/DMSO) δ 7.29 (s, 1H), 4.11 (dd, 2H), 3.62 (dd, 2H), 3.55 (s, 3H), 3.29 (s, 3H).

^{1}H NMR of **Zn50Cu50** (200 MHz, DCl/D_2O/DMSO) δ 7.29 (s, 1H), 4.10 (s, 2H), 3.59 (s, 5H), 3.29 (s, 3H).

^{1}H NMR of **Zn25Cu75** (200 MHz, DCl/D_2O/DMSO) δ 7.27 (s, 1H), 4.08 (s, 2H), 3.60 (s, 5H), 3.27 (s, 3H).

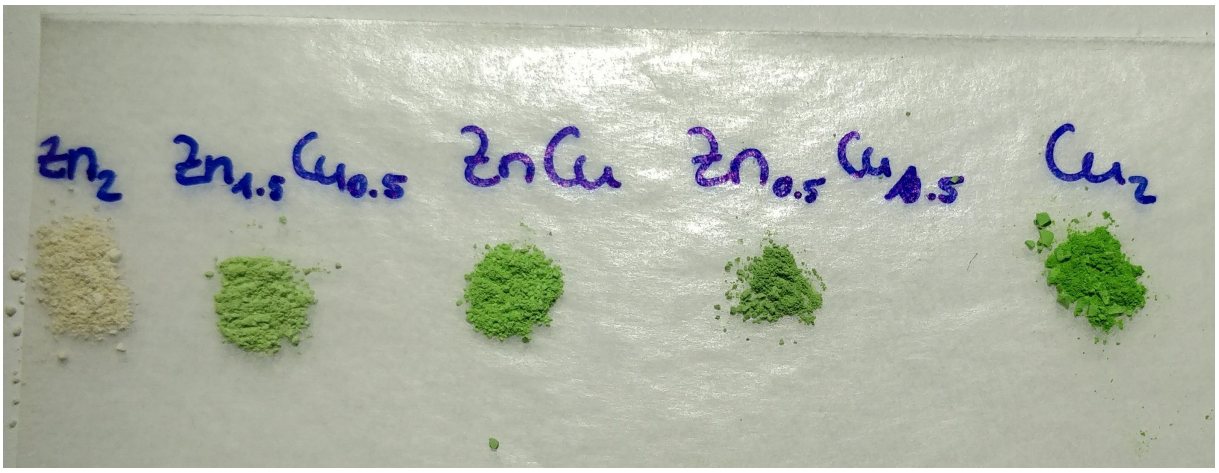

Figure S1: Photographs of the prepared materials (from left to right) **Zn100**, **Zn75Cu25**, **Zn50Cu50**, **Zn25Cu75** and **Cu100**.

S2 NMR Spectra of digested MOFs

Liquid phase NMR (nuclear magnetic resonance) spectra were measured on a Bruker Avance DPX 200 spectrometer (1H, 200 MHz) at 293 K. ^{1}H NMR spectra of digested MOFs were recorded in 0.5 ml DMSO-d_6 and 0.05 ml of DCl/D_2O (20%). Chemical shifts are given relative to TMS (Tetramethylsilane) and are referenced to the solvent signals as internal standards.

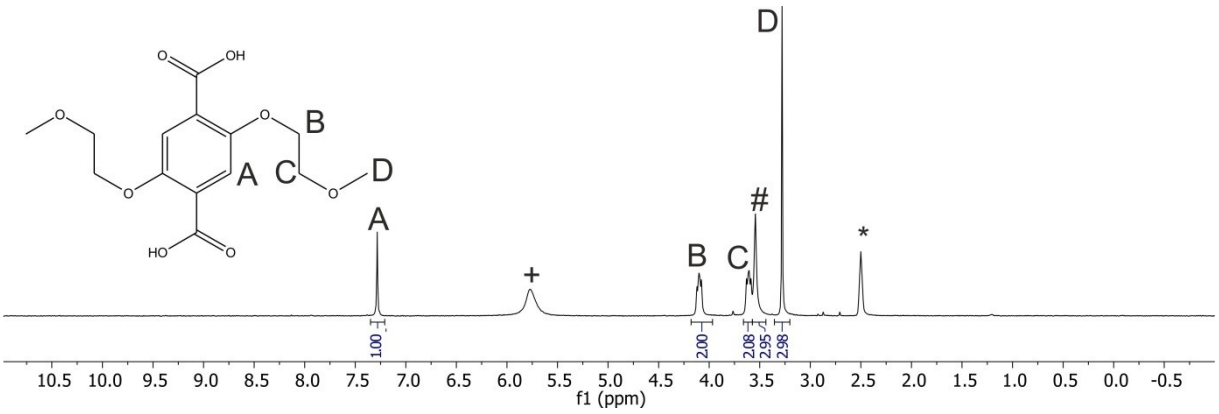

Figure S2: ^{1}H-NMR of **Zn75Cu25** after digestion in DMSO/DCl/D_2O. The signal marked with an asterisk marks the DMSO-d_6 and the + belongs to D_2O/DCl. The hash marks the dabco signal.

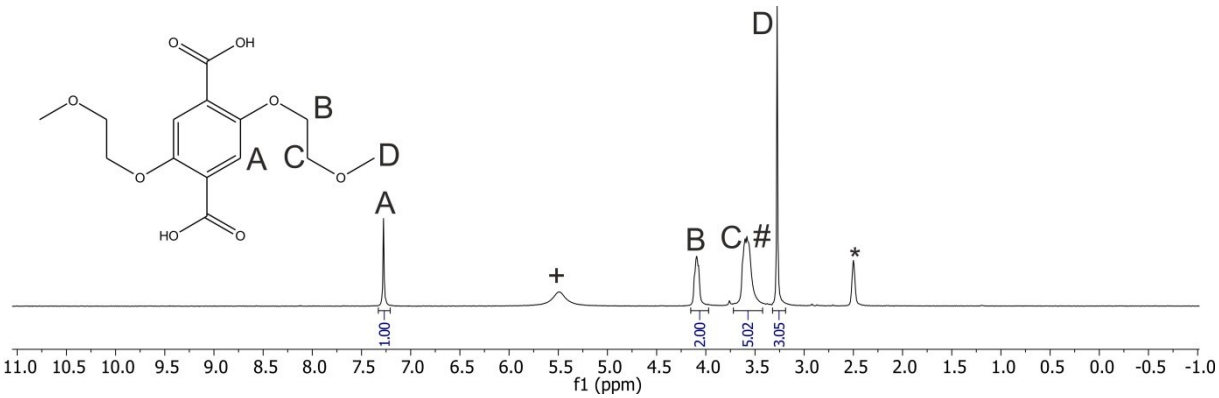

Figure S3: ^{1}H-NMR of **Zn50Cu50** after digestion in DMSO/DCl/D_2O. The signal marked with an asterisk marks the DMSO-d_6 and the + belongs to D_2O/DCl. The hash marks the dabco signal.

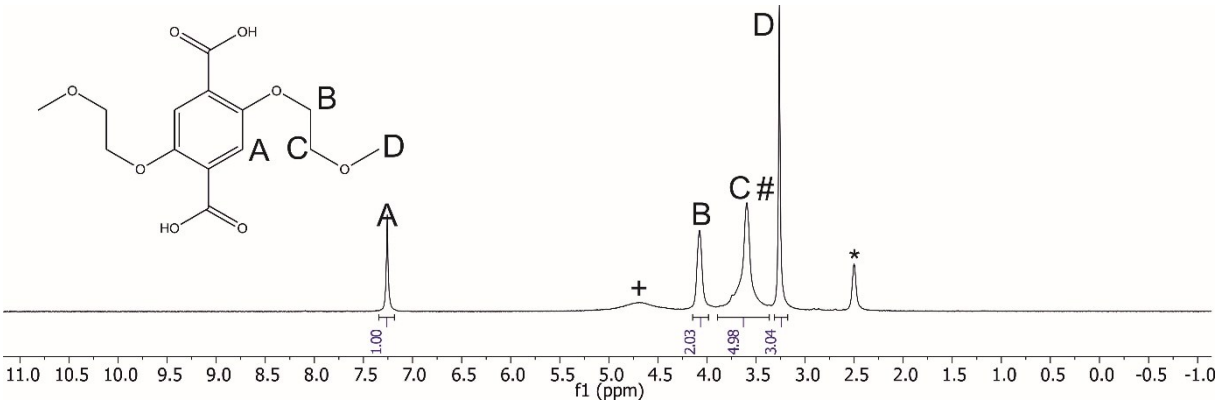

Figure S4: ^{1}H-NMR of **Zn25Cu75** after digestion in DMSO/DCl/D_2O. The signal marked with an asterisk marks the DMSO-d_6 and the + belongs to D_2O/DCl. The hash marks the dabco signal.

S3 IR Spectra

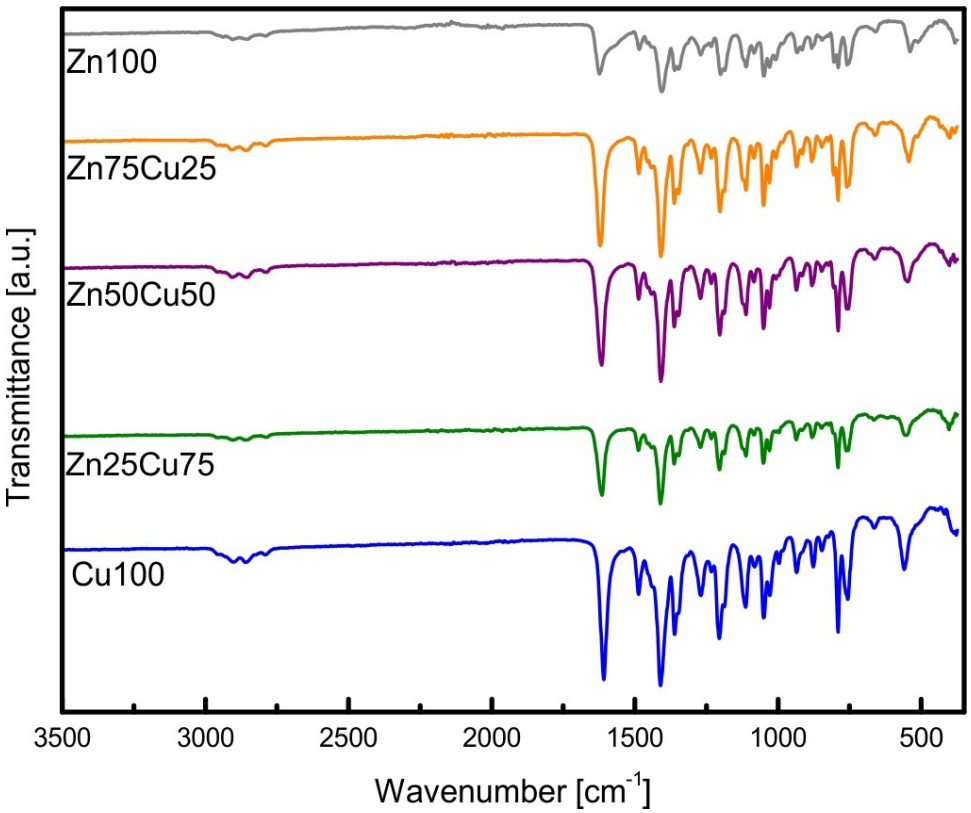

Figure S5: FTIR spectra of the activated materials **Zn100** (grey), **Zn75Cu25** (orange), **Zn50Cu50** (purple), **Zn25Cu75** (green), and **Cu100** (blue).

S4 Thermogravimetric Analysis

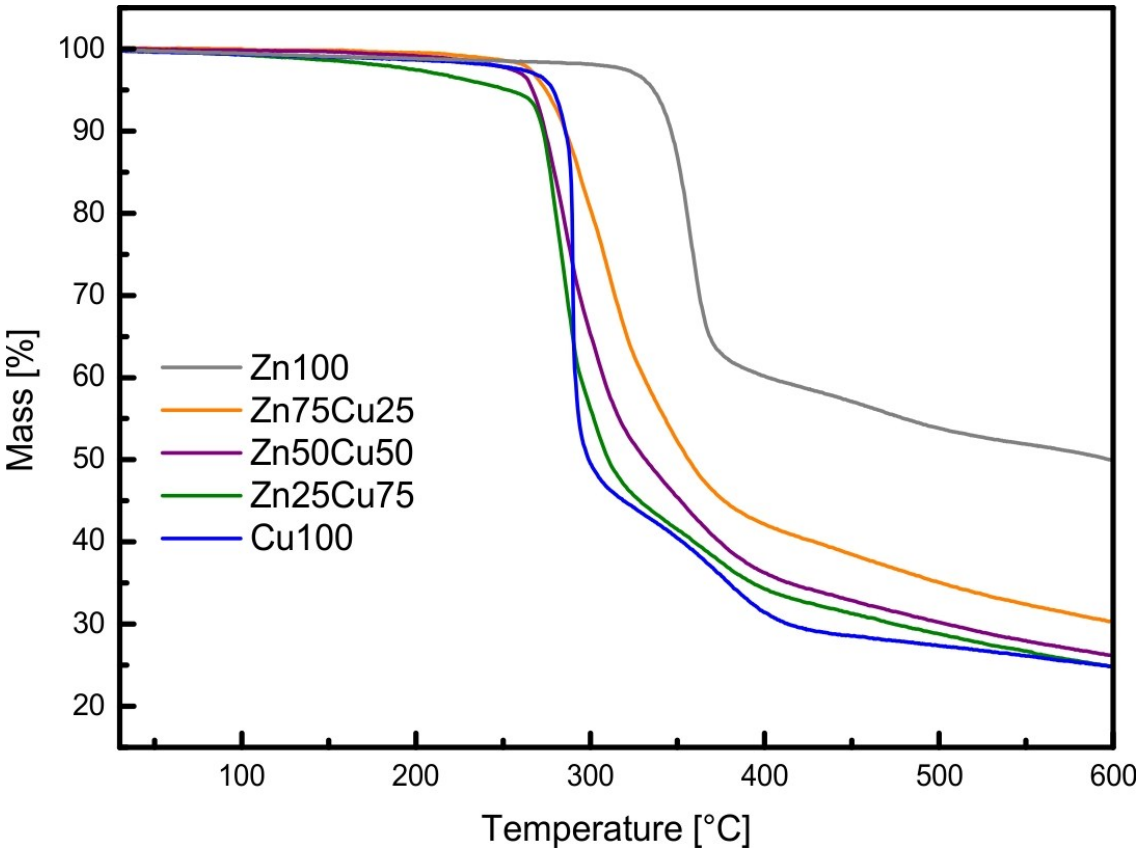

Figure S6: TG traces of the activated materials **Zn100** (grey), **Zn75Cu25** (orange), **Zn50Cu50** (purple), **Zn25Cu75** (green), and **Cu100** (blue).

S5 Powder X-Ray Diffraction and Cell Refinements

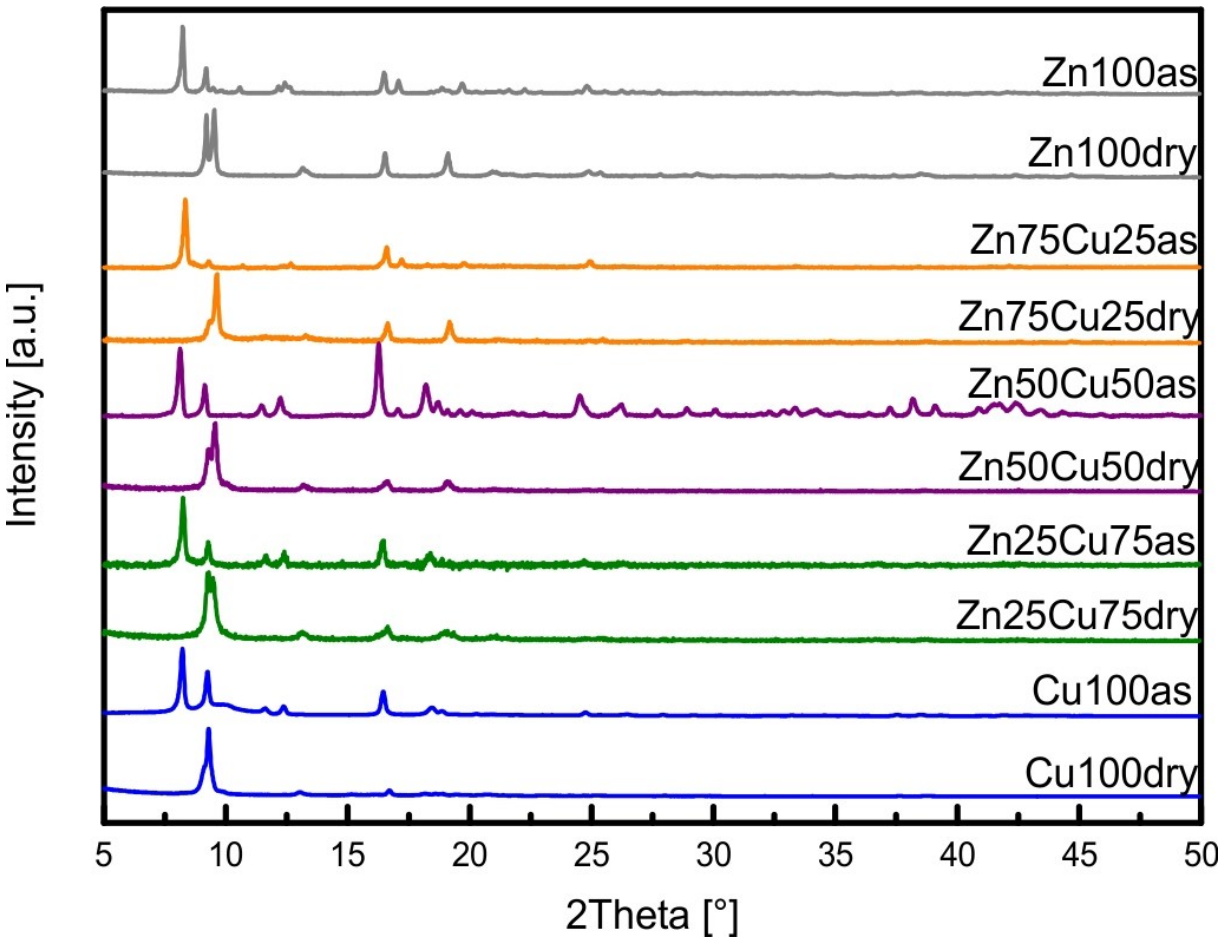

Figure S7: PXRD patterns of the as-synthesized (as) and activated materials (dry) **Zn100** (grey), **Zn75Cu25** (orange), **Zn50Cu50** (purple), **Zn25Cu75** (green), and **Cu100** (blue).

Pawley fits were performed for each sample using the software package GSAS-II Version 3334.[2] The dried samples exhibit the space group *C*2/*m* consistently across the range of compositions. The as-synthesized Zn-rich samples are best fit to the monoclinic space group *C*2/*m*, but a transition takes place as the samples become more Cu-rich to tetragonal *P*4/*mmm*. For each sample peak shape parameters are refined using both Gaussian (U,V,W) and Lorentzian (X,Y) functions. The zero-point shift was also refined for all samples. The final fits show decent matching between the calculated fits and the XRD patterns with low R_{wp} values. It is clear that there is a slight unidentified impurity that can be seen in the dried Zn-rich samples, but this is not expected to have an effect on the lattice constant derived from the Pawley fit.

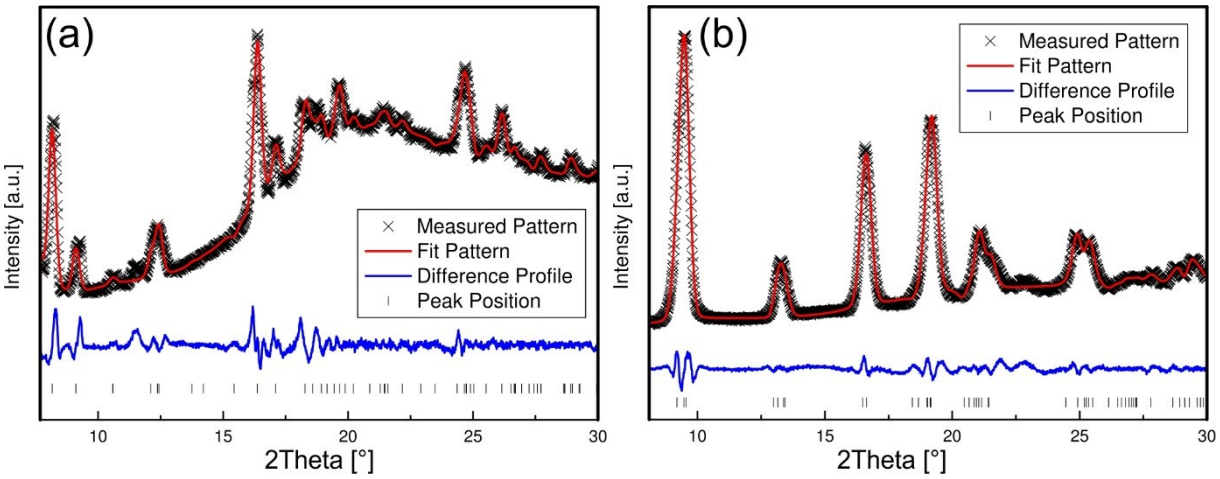

Figure S8: Pawley fits to the diffraction patterns of **Zn75Cu25as** (a) and **Zn75Cu25dry** (b). Black crosses represent the experimental data and red lines represent the fit. The difference profile is shown in blue. Black ticks mark the positions of the Bragg reflections. The patterns were measured on the in-house diffractometer (λ = 1.5418 Å).

Compound	**Zn75Cu25as**	**Zn75Cu25dry**
space group	C2/m	C2/m
a / Å	16.689(3)	18.678(7)
b / Å	14.214(3)	10.653(3)
c / Å	9.700(3)	9.623(3)
β / °	91.90(2)	91.90(4)
V / Å^3	2299.7(7)	1913.5(14)
Z	2	2
Red. V / Å^3	1149.85	956.75
Rwp	2.93	2.64

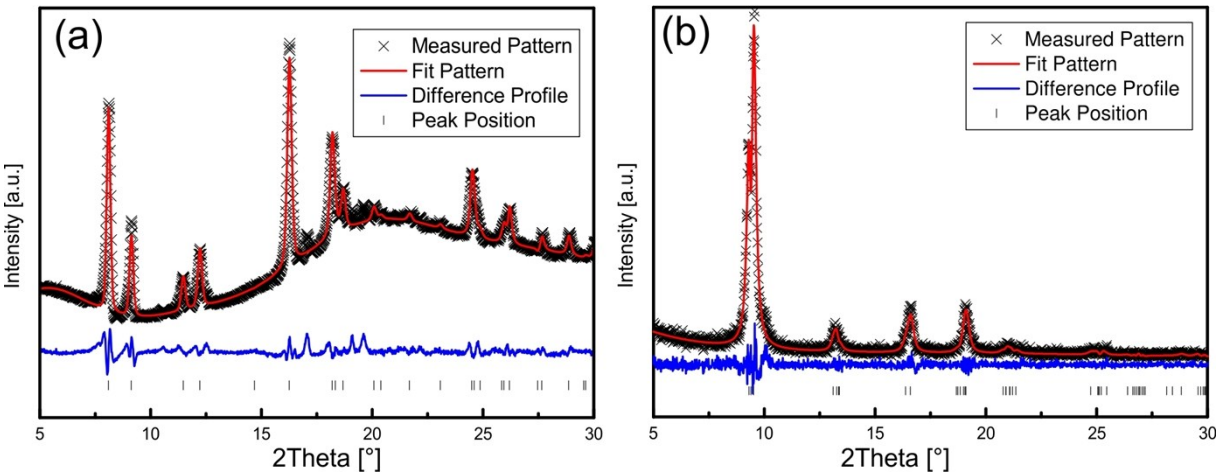

Figure S9: Pawley fits to the diffraction patterns of **Zn50Cu50as** (a) and **Zn50Cu50dry** (b). Black crosses represent the experimental data and red lines represent the fit. The difference profile is shown in blue. Black ticks mark the positions of the Bragg reflections. The patterns were measured on the in-house diffractometer (λ = 1.5418 Å)**.**

Compound	**Zn50Cu50as**	**Zn50Cu50dry**
space group	*P*4/*mmm*	*C*2/*m*
a / Å	10.8835(12)	18.612(6)
b / Å	10.8835(12)	10.658(4)
c / Å	9.6616(15)	9.558(3)
β / °	90	90.40(2)
V / Å^3	1144.4(4)	1895.9(13)
Z	1	2
Red. V / Å^3	1144.4	947.95
Rwp	3.45	6.29

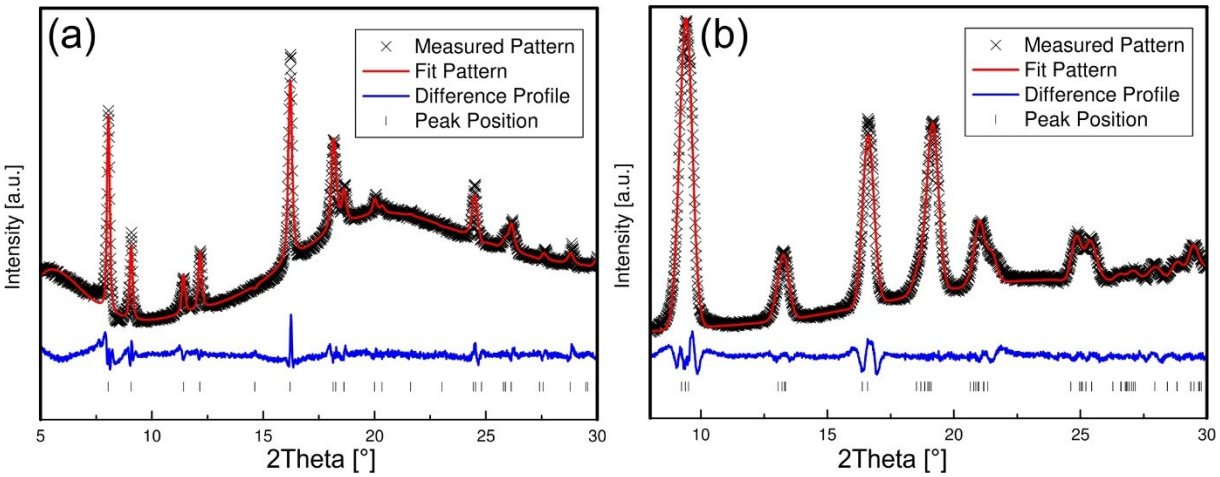

Figure S10: Pawley fits to the diffraction patterns of **$Zn_{25}Cu_{75}$as** (a) and **$Zn_{25}Cu_{75}$dry** (b). Black crosses represent the experimental data and red lines represent the fit. The difference profile is shown in blue. Black ticks mark the positions of the Bragg reflections. The patterns were measured on the in-house diffractometer (λ = 1.5418 Å)**.**

Compound	**Zn25Cu75as**	**Zn25Cu75dry**
space group	*P*4/*mmm*	*C*2/*m*
a / Å	10.8629(12)	18.817(17)
b / Å	10.8629(12)	10.677(2)
c / Å	9.6527(14)	9.571(6)
β / °	90	91.12(6)
V / Å^3	1139.0(4)	1922(2)
Z	1	2
Red. V / Å^3	1139	961
Rwp	2.98	3.5

S6 SEM-EDX of Mixed Metal MOFs

Table S2: Zn:Cu Ratios in the samples determined by EDX Mapping.

Sample	Zn [%] (theo.)	Cu [%] (theo.)	Zn [%] (SEM-EDX)	Cu [%] SEM-EDX
Zn75Cu25	75	25	76.30	23.70
Zn50Cu50	50	50	55.38	44.62
Zn25Cu75	25	75	24.00	76.00

S7 Nitrogen Sorption Isotherms

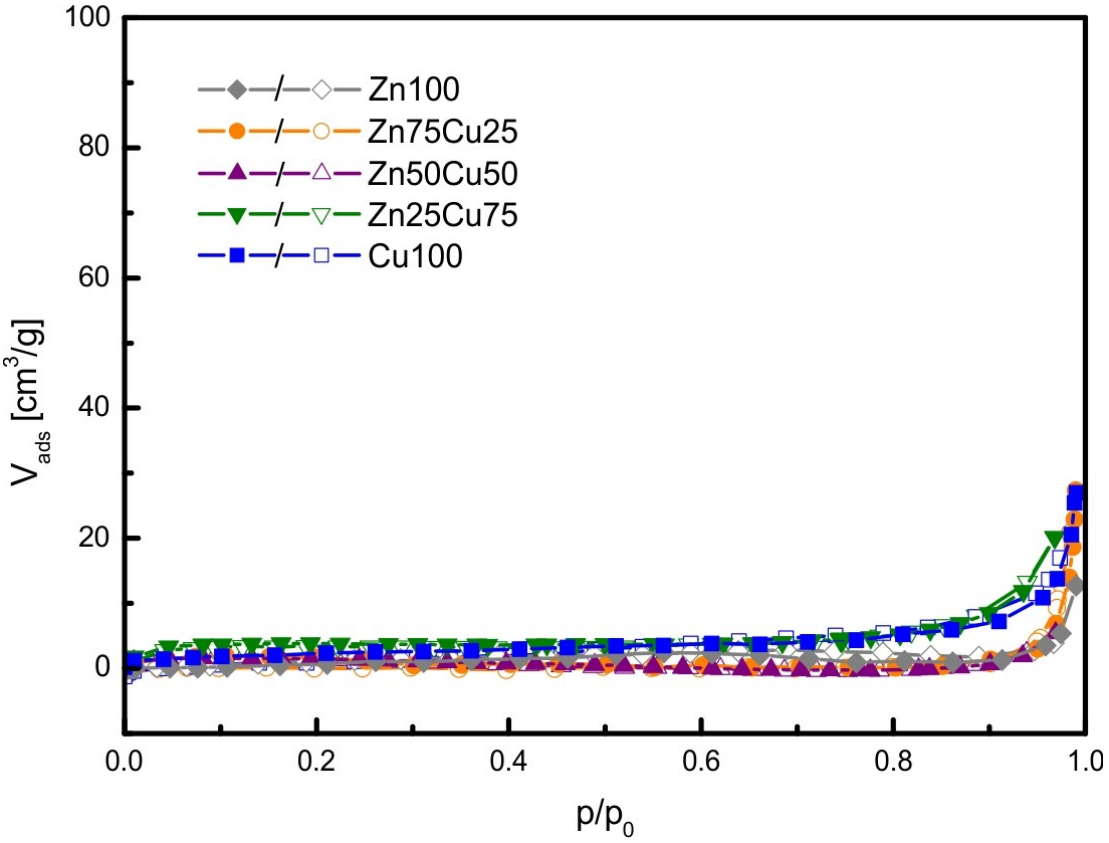

Figure S11: N_2 sorption isotherms of the activated materials **Zn100** (grey diamonds), **Zn75Cu25** (orange circles), **Zn50Cu50** (purple triangles), **Zn25Cu75** (green triangles), and **Cu100** (blue squares) conducted at 77 K.

S8 Differential Scanning Calorimetrie

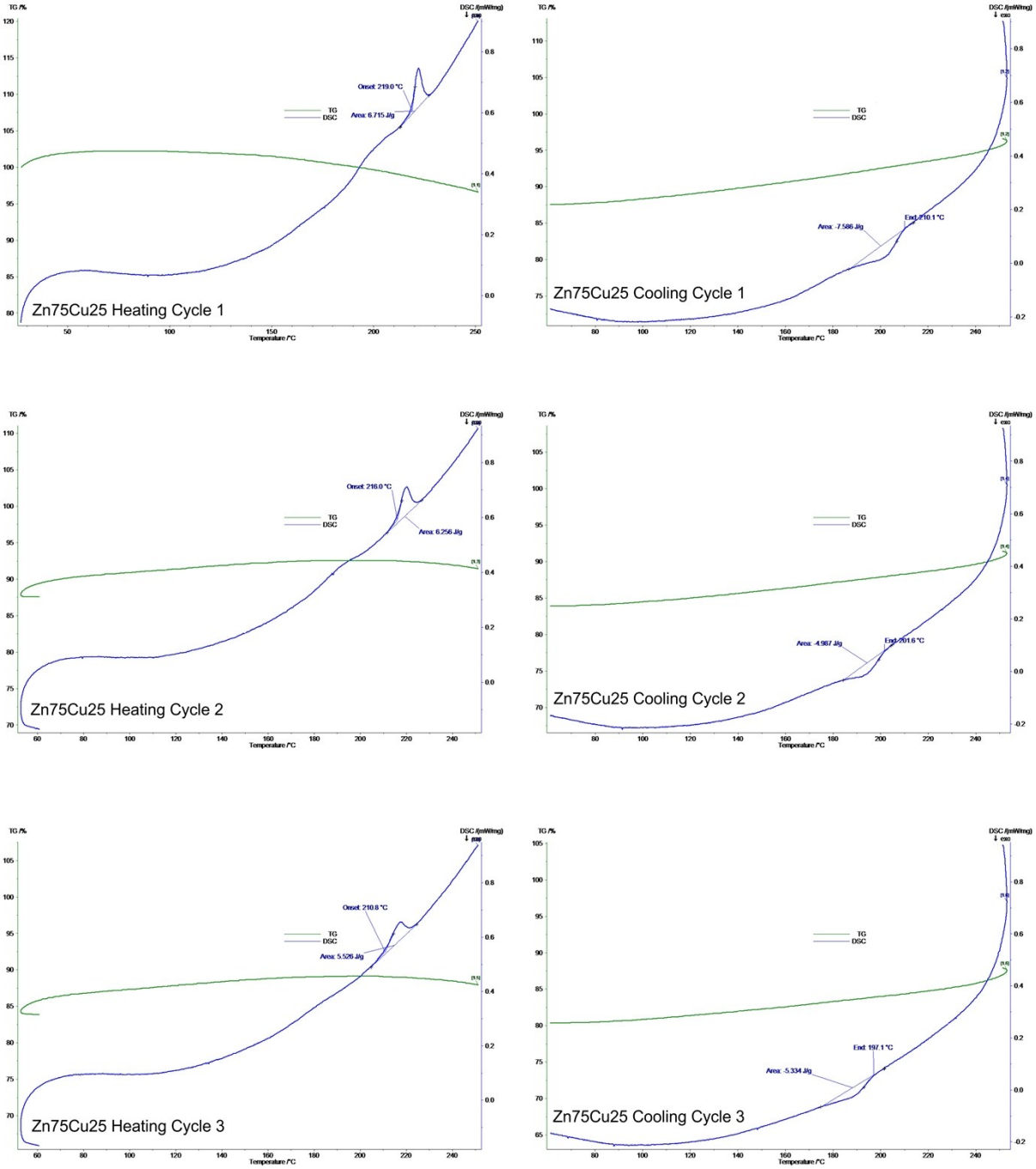

Figure S12: TG-DSC measurements of **Zn75Cu25dry**. Blue and green curves represent the mass (in %) and the heat flux (in mW/mg). Peak onsets and areas for the heat signatures of the phase transitions are displayed in the DSC curves.

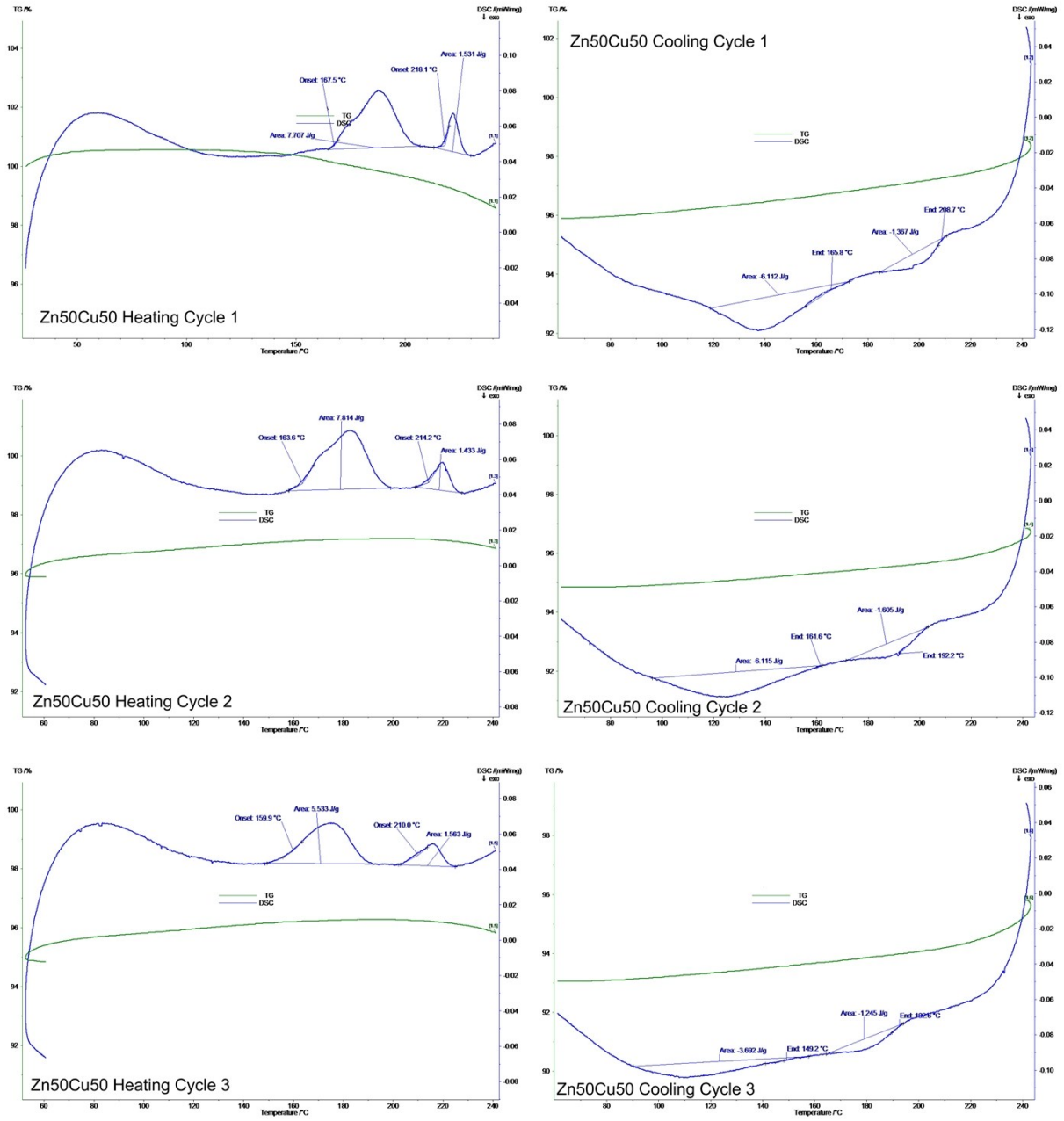

Figure S13: TG-DSC measurements of **Zn50Cu50dry**. Blue and green curves represent the mass (in %) and the heat flux (in mW/mg). Peak onsets and areas for the heat signatures of the phase transitions are displayed in the DSC curves.

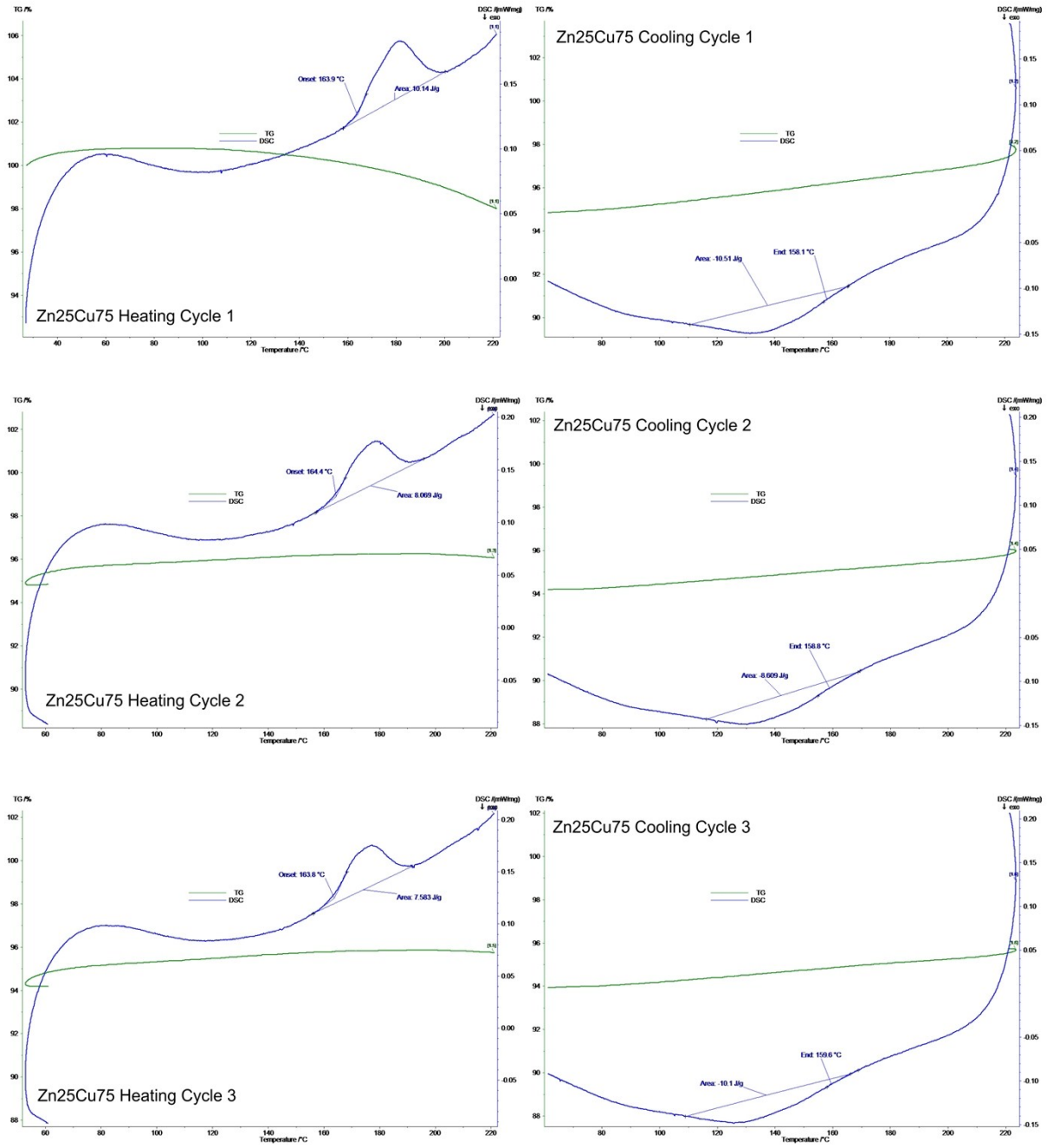

Figure S14: TG-DSC measurements of **Zn25Cu75dry**. Blue and green curves represent the mass (in %) and the heat flux (in mW/mg). Peak onsets and areas for the heat signatures of the phase transitions are displayed in the DSC curves.

S9 Additional Pair Distribution Function Plots

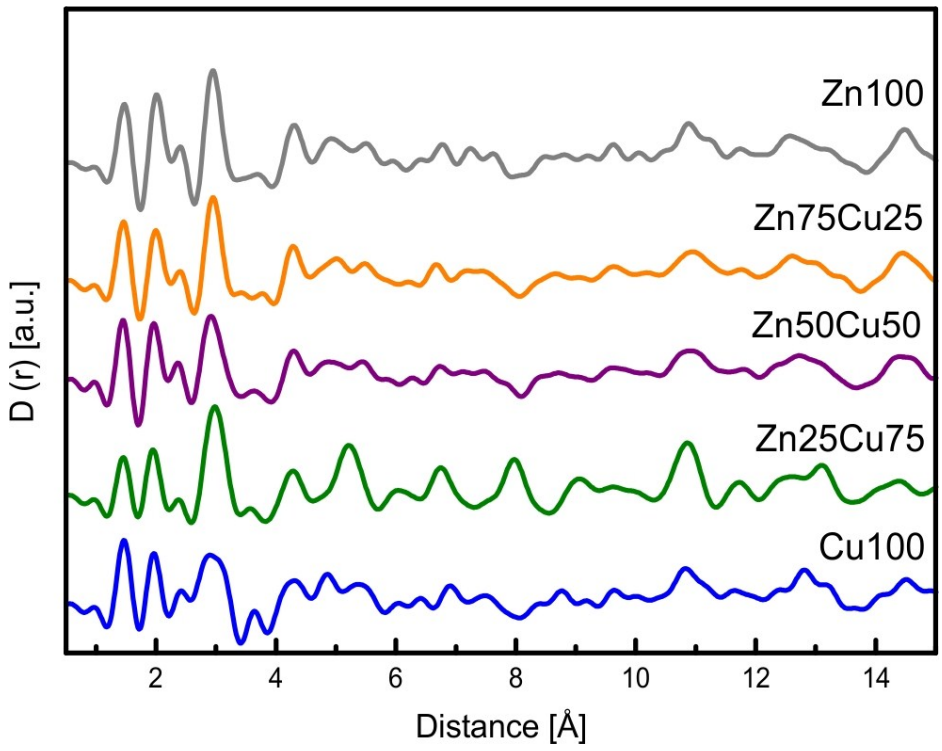

Figure S15: Full range of the total scattering derived Pair Distribution Functions for the narrow pore phases of **Zn100** (grey), **Zn75Cu25** (orange), **Zn50Cu50** (purple), **Zn25Cu75** (green) and **Cu100** (blue)

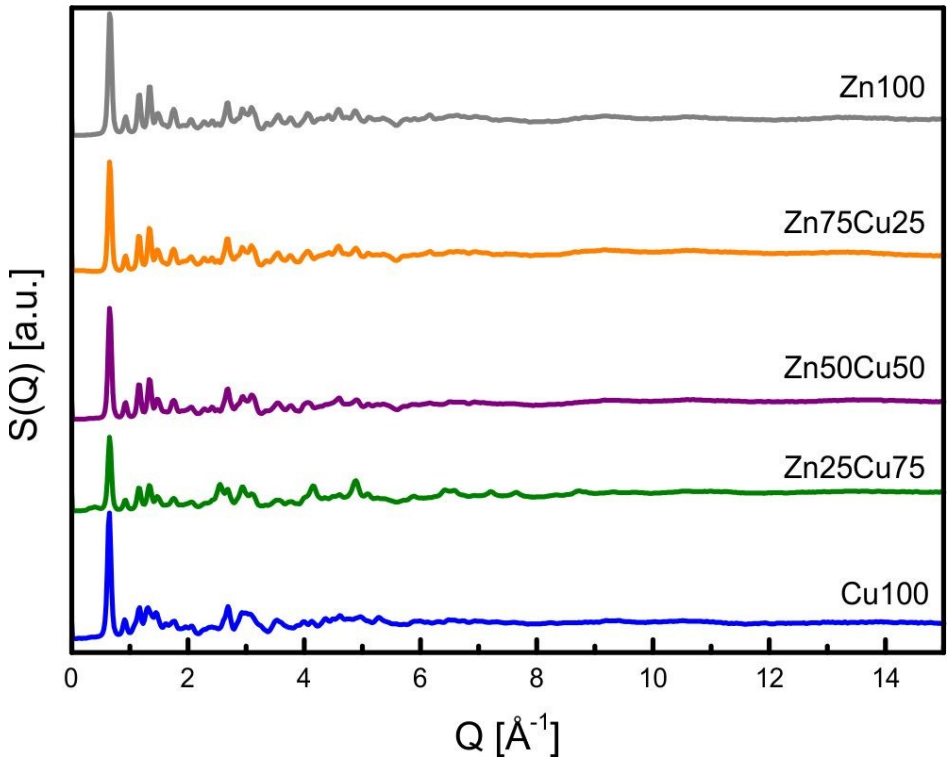

Figure S16: Total scattering derived X-ray scattering factors for the narrow pore phases of **Zn100** (grey), **Zn75Cu25** (orange), **Zn50Cu50** (purple), **Zn25Cu75** (green) and **Cu100** (blue)

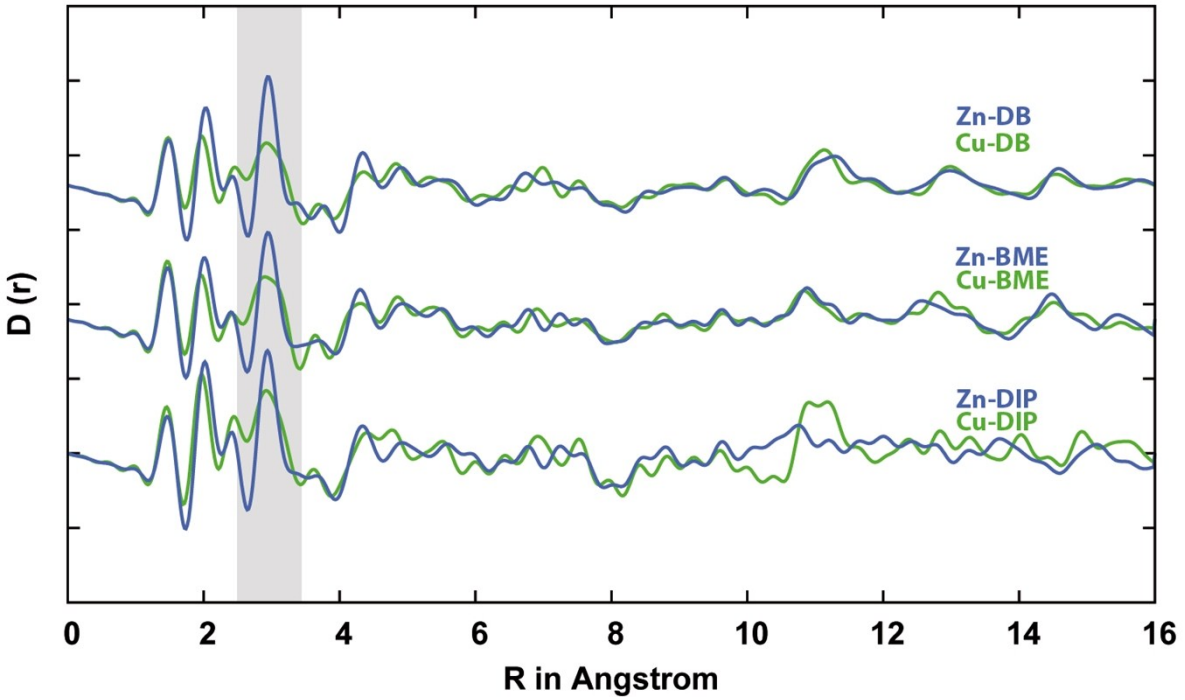

Figure S17: Total X-ray Scattering derived pair distribution functions for a range of Cu^{2+} and Zn^{2+} Paddlewheel MOFs in the narrow pore state, highlighting the broadening of the peak representing the Cu-Cu distances in all cases compared to the Zn-Zn distance. **Zn-DB** and **Cu-DB** represent M_2(DB-bdc)$_2$(dabco) phases, **Zn-BME** and **Cu-BME** represent M_2(BME-bdc)$_2$(dabco)and **Zn-DIP** and **Cu-DIP** represent M_2(DiP-bdc)$_2$(dabco) (with DB-bdc^{2-} = 2,5-Dibutoxy-1,4-benzenedicarboxylate and DiP-bdc^{2-} = 2,5-Diisopropoxy-1,4-benzenedicarboxylate)

S10 References

(1) Henke, S.; Schneemann, A.; Wuetscher, A.; Fischer, R. A. Directing the Breathing Behavior of Pillared-Layered Metal-Organic Frameworks via a Systematic Library of Functionalized Linkers Bearing Flexible Substituents *J. Am. Chem. Soc.* **2012**, *134*, 9464.

(2) Toby, B. H.; Von Dreele, R. B. GSAS-II: the genesis of a modern open-source all purpose crystallography software package *J. Appl. Crystallogr.* **2013**, *46*, 544.